Infrasound from Tornados: Theory, Measurement, and Prospects for Their Use in Early Warning Systems

Carrick Talmadge

Postal:
National Center for Physical Acoustics
University of Mississippi
University, MS 38677
USA

Email:
clt@olemiss.edu

Roger Waxler

Postal:
National Center for Physical Acoustics
University of Mississippi
University, MS 38677
USA

Email:
rwax@olemiss.edu

Tornados may produce a low-frequency signature that could be used in automatic warning systems.

Introduction

Infrasound is propagating sound waves with frequencies below the range of human hearing. A practical frequency range for infrasound that will propagate over long distances is 0.01-20 Hz. The lower frequency cut off for propagating infrasound arises because the buoyancy of parcels of air becomes comparable to the pressure gradient forces of acoustic waves at sufficiently low frequencies. The precise frequency for this cut off occurs at the Brunt–Väisälä frequency (Stull, 1995), the exact value of which depends on details of the vertical profile of the atmosphere.

One of the more famous examples of long-range propagating infrasound is the explosive eruption of Krakatoa Volcano in Indonesia. Audible sounds were heard as far away as 5,000 km, and low-frequency infrasound signals with periods greater than one minute were propagated around the Earth at least seven full times (e.g., Fee and Matoza, 2013).

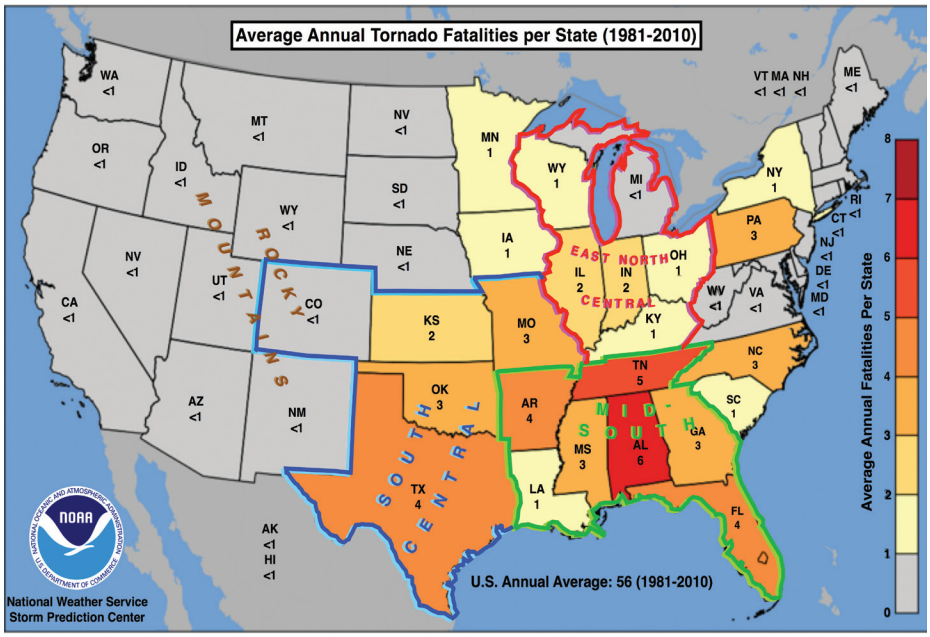

Figure 1. *Annual average death rate from tornados. Also shown are the geographical regions referred to in the text. Note that these geographical regions correspond approximately to tornado climatological zones rather than to traditional geographical regions. Adapted from original figure by The National Oceanic and Atmospheric Administration (NOAA).*

Because infrasound propagates for long ranges, it can be used for hazard monitoring. For volcanic warnings, atmospheric blasts can be detected by infrasound stations even when the peak of the volcano is obscured by clouds so that optical observations are not possible. Another important infrasound source is hurricanes, which produce characteristic tonelike signals called "microbaroms" produced by

the nonlinear interaction between ocean waves and the atmosphere (Waxler and Gilbert, 2006). It was reported by Raveloson et al. (2012) that infrasound signals from the 2011 Tohoku-Oki, Japan, earthquake could have been used as an early warning of the impending tsunami.

Tornados represent one of the most common natural hazards posed in the United States. Within any given year, on average, some 800 tornados will occur within the United States east of the Rockies, resulting in 80 deaths and 1,500 injuries [National Oceanic and Atmospheric Administration (NOAA) National Severe Storms Laboratory]. In spite of the mystique associated with "Tornado Alley" (typically listed as the states of Oklahoma, Kansas, and Nebraska as well as adjoining areas from neighboring states), southern states, including Mississippi, remain a primary target for tornadic activity. These regions are shown in **Figure 1.**

Even with recent advances in Doppler radar technology and other early warning systems, tornados in the central regions of the United States remain a significant risk for injury or loss of life. Augmenting existing detection arrays with infrasound/low-frequency arrays offers a possible new method for improving the safety of people living in high-risk tornado areas.

We focus here on the possible generation of infrasound from tornados and detection of these waves on a regional scale (i.e., over distances up to 100 km from the source). For this distance scale, the main influences on infrasound propagation are the distance of the source and the effective vertical atmospheric sound-speed profile in the direction of propagation (e.g., Attenborough et al., 2006). In a (theoretical) atmosphere with a constant vertical sound speed, sound intensity decreases as the inverse square of the propagation distance. For "downwind" propagation—known as "ducted" propagation—sound intensity decreases inversely with distance. Hence it is important for long-distance propagation measurements to place the arrays downwind from the infrasound source when possible.

In this paper, we start by discussing the mechanisms for tornado genesis. We then review the hazards associated with tornados, noting that while the Great Plains (a grassland prairie east of the Rocky Mountains that extends from the southern US border into Canada) have received much of the attention for tornadic research, there is a substantial safety risk from tornados in the "US Mid-South" (**Figure 1**). We then discuss evidence that tornado vortices produce infrasound and low-frequency sound. We review the results from our recent tornadic thunderstorm measurements in Oklahoma (Frazier et al., 2014). Finally, we show that there are characteristic signals that seem to be present only when tornados have touched down. It is possible that these characteristic signals could be used to augment existing early warning systems and lead to an improvement in safety for people at risk from tornadic thunderstorms.

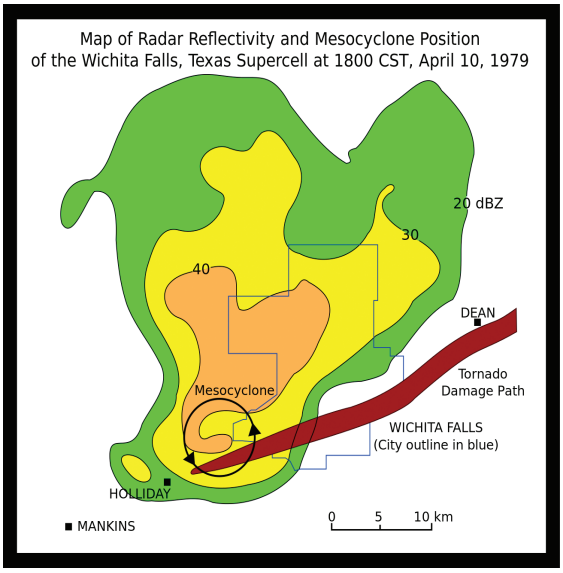

Figure 2. *Radar reflectivity for the Texas supercell over Wichita Falls, TX on April 11,1979. The location of the mesocyclone is shown by the circle, which is oriented over the hook region of the storm. Obtained from NOAA, Don Burgess, OSF, and Vanessa Ezekowitz.*

Tornado Genesis

There are two generally accepted patterns for energetic tornado generation (reviewed in Bluestein, 1999). The first is associated with supercell thunderstorms (storms that are large, typically 15 km wide by 15 km tall) that have a deep, continuously rotating updraft known as the mesocyclone. Tornados from supercells are the most studied class of tornados due to the relative predictability of where a tornado will appear within the supercell (the "hook region" in **Figure 2**). These are also studied in part because of the visibility of supercells, which often have localized precipitation zones separated from the mesocyclone (a large region of rotation within a thunderstorm) and because of the geographical accessibility of the Great Plains region where many of this type of storm occur. Supercells are noted for producing the most intense and dangerous tornados, with nearly half of all fatalities occurring from these intense storms. However, even with their relatively well-defined structure, current radar algorithms achieve less than a 50% probability of detection for acceptable levels of a false alarm rate (Mitchell, 1998).

The other mechanism for tornado genesis is simply referred to as "non-supercell." Typically, these tornados are associ-

ated with less organized storm systems, in which precipitation bands shroud the region of formation of the tornado. Tornados generated by this mechanism tend to be weaker, but they are very dangerous due to their lack of predictability and the poor visibility associated with the phenomenon. Roughly one half of the storms in the Southeastern United States are of this variety, with almost 100% of the tornados spawned in Florida being non-supercell in origin (Kelly et al., 1978).

Tornado Alley

Tornados in the US Plains States represent an all too familiar threat to life, health, and property. What is not typically well appreciated is that the area that has the largest threat for loss of life is the United States Mid-South. Contributors to the higher mortality rate include rain-wrapped thunderstorms, which obscure tornados within the storm cell as well more convoluted terrain and the presence of tall forests that obscure the horizon. Without advanced warning from the emergency broadcast system that provides alerts to oncoming tornados, people who live in rural areas in these states are subject to the whims of nature.

In the Great Plains, low-precipitation supercells are a relatively common occurrence (Bluestein, 1999). Because of the lack of significant precipitation, very clear views of tornadic activity are usually possible, making them ideal for the study of tornados. The relatively smooth terrain and lack of tall forests also allow views to the horizon in many cases.

In **Figure 3** we show histograms of the total number of tornados for each day over the period 1950–2009 summed over the South-Central and over the Mid-South regions (as defined in **Figure 1**). These figures show that the tornado season is roughly concentrated in the band from days 80–180 of the year (mid-March through the end of June of each year). For the Mid-South, there is strong activity from January through March but also late season activity in November and December.

The relatively narrow window for tornadic activity and a safer operating environment, due to good visibility and road systems that are on a regular grid, make the South-Central region the preferred region for tornado research and tornado chasing. The downside of this circumstance is that most research on tornado genesis arises from data obtained from low-precipitation supercells, and tornado genesis from high-precipitation supercells and front boundaries (more common in the Mid-South) tend to be understudied (which ultimately may contribute to the higher mortality rates recorded in the Mid-South).

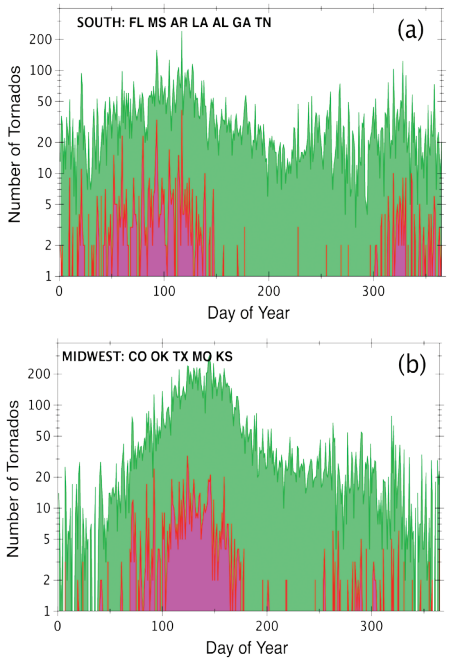

Figure 3. *Histogram of tornadic events for (a) the "Mid-South" geographical region and (b) the "South-Central" geographical region. The states used for each region are shown by their state abbreviations. The green shaded area is for all tornadoes, and the magenta area is for just violent (EF3-EF5) tornados.*

In spite of the South-Central region's deserved reputation for having a high rate of tornados, we see that the Mid-South has nearly identical rates for tornados as the South-Central, and both the East-North-Central (**Figure 1**) and Mid-South regions suffer higher fatality rates than does the South-Central region. Lower visibility due to terrain, presence of trees, and a higher frequency of rain-wrapped tornados are likely contributors to these higher fatality rates. Possibly the fact that Plains States tornados and the meteorological factors associated with their genesis are well-studied has reduced the risk of fatality associated with South-Central tornados.

Infrasound from Tornados

Since the early 1970s, convective systems have been known to be sources of infrasound (e.g., Bedard and Georges, 2000). The typical frequency band for these sounds is about 0.017 –1 Hz (Georges, 1973). However, there is a great deal of uncertainty about the origins and significance of the sounds. A variety of potential source mechanisms have been proposed for infrasound generated by convective storms. Georges (1976) considered many of these and concluded that vortex motion was the most plausible candidate. While the suggestion has been made that these signals are a precursor to tornadic activity, Bedard (2005) concluded that "it seems unlikely that the much lower frequencies detected by these geoacoustic observatories had any direct connection with tornado formation."

The first published accounts of sound recordings from a tornado were by Arnold et al. (1976). These data were restricted to the frequency range from 100–2,000 Hz. All measurements were collected using low-quality analog equipment, which led to significant distortion of the measured signal. The main findings were that the measured signal was broadband in character, with a roll-off above 500-Hz, and the band start frequency was associated with the lower frequency cut off of the measuring equipment.

More recently Bedard (2005) has reported on measurements of infrasound by a four-element array of sensors in the 0.5–10 Hz band from tornadic thunderstorms and concluded that the 0.5–2.5 Hz band contained the maximum correlation between sensors. Note that this result is dependent on the sensor separation, the atmospheric noise field at the time of the measurements, and characteristics of the sensors (such as its frequency response and noise floor), as well as on the characteristics of the infrasound signal at the array. It was suggested that this signal was associated with the tornadic activity, but the mechanisms for its creation remain unclear. For example, Abdullah (1966) proposed a mechanism based on radial oscillations of the tornado vortex; however, Shecter (2012) demonstrated that this mechanism was implausible. Other possible mechanisms include turbulent flow associated with the tornado vortex and interactions between the tornado and the ground.

If tornados were known to produce infrasound or low-frequency signals, and if these signals had characteristic features, infrasound arrays could be used to augment existing early warning systems and possibly significantly improve the safety of individuals living in high-risk areas for tornados. However, previous results do not unequivocally establish that tornados produce infrasound nor do they provide any characteristics of the signal that are unique to tornados that have touched down. As part of a program on hazards monitoring that were funded by NOAA, the National Center for Physical Acoustics (NCPA) and Hyperion Technology Group Inc. conducted a series of infrasound sensor deployments in Oklahoma over the summer of 2011. The primary interest in this deployment was to address both of those issues.

Data Collection

The NCPA, in collaboration with Hyperion Technology Group Inc., collected data for two tornado outbreaks on May 24, 2011, and June 11, 2011. The sensors used for these measurements were a new class of digital infrasound sensor (**Figure 4**) developed at the NCPA. These sensors have a built-in 24-bit digitizer with GPS time syncing and 802.11/b wireless connectivity.

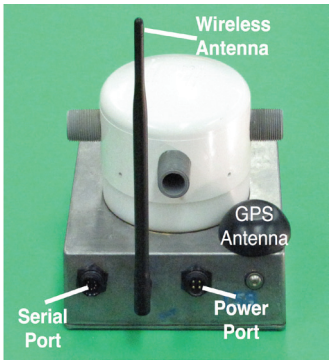

Figure 4. *Digital NCPA sensor (for scale, floor tiles 1 foot × 1 foot in size). The sensor is GPS synchronized, 1000 samples/second, (22.5 noise free bits).*

The NCPA sensors have a unique capability to measure signals from infrasound to low-frequency acoustics (0.015-500 Hz). The frequency response of this sensor was from 0.001-100 Hz (**Figure 5**), and its gain was set so that the maximum transducible pressure amplitude was about 90 Pa. For this exercise, the sensor sampling rate was set to 1,000 samples/second.

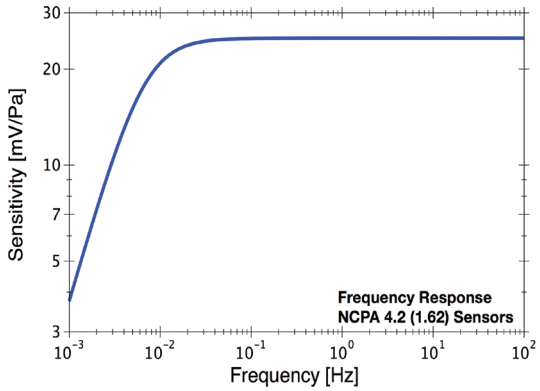

Figure 5. *Nominal sensitivity curve for the NCPA microphones used in this deployment. This sensitivity function has an asymptotic value of 25 mV/Pa, a pole at 6.4 mHz, and a zero at the origin.*

Oklahoma Campaign

Oklahoma was targeted for this project because the storm-chasing season lasts for a shorter period. As mentioned previously, the relative flat terrain coupled with the absence of standing forests offers improved visibility and a reduced risk of unintentional tornado intercepts. One of the objectives of this deployment was to obtain broadband signals from tornados by placing sensors in the region of tornadogenic storms. In some cases, sensors were placed within a few kilometers of the path of very large tornados (EF4 and EF5), but this was not a primary goal of the project.

The second and primary objective was to deploy regional arrays northeast of the tornadic convective storm. The northeast direction was chosen because this is the direction

of travel of the tornados and, in principle, would allow observation of the tornado from its touchdown location and along the path of the tornado as the tornado approached the regional array. We would expect sound ducting to also be dominantly in the northeast direction.

In order to simplify the installation process, the array elements should be equally spaced on public easements along roads. The spacing was chosen to be 1 km based on the reported infrasound by Bedard (2005) in the 0.5-2.5 Hz band. This spacing turned out to be too large because no infrasound below a few hertz was observed in this deployment.

The sensor deployment consisted of two teams of researchers from Hyperion Inc.: one that would be responsible for the regional arrays and a second that would aim for near-field intercepts of tornados. The locations of the arrays were selected based on severe weather forecasting.

The findings of this study are reported in Frazier et al. (2014). Here we summarize the main results, focusing on data and observations that point to the tornado vortex as the main candidate for the source of the infrasound and low frequency reported in Frazier et al. (2014).

May 24, 2011, Oklahoma Outbreak

The May 24, 2011, outbreak, was part of a series of violent weather events that extended from May 11–26. During this period, a total of 244 tornados were recorded in 12 states, of which two were EF-5 (>200 mph estimated winds), three were EF-4 (166–200 mph estimated winds) and eight were EF-3 (115–135 mph estimated winds) in strength (https://www.ncdc.noaa.gov/data-access/severe-weather). This outbreak included the deadly May 22 tornado in Joplin, Missouri. During this outbreak there were 178 fatalities and 1,629 reported injuries associated with tornadic activity and the economic damage from this outbreak exceeded $7 billion US (Buhayar, 2011). A Google Earth KML file of the tornado track data is provided at http://www.srh.noaa.gov/oun/?n=events-20110524.

The major tornados in Oklahoma during the May 24, 2011, outbreak are shown in **Table 1**. Tracks associated with tornado intercepts are shown in **Figure 6** together with the array locations where data were collected for these events. As can be seen, this deployment was highly successful in locating arrays in both the near field for the Chickasha-Blanchard-Newcastle (CBN) tornado, and regionally for the Calumet-El Reno-Piedmont-Guthrie (CPEG) and Stillwater (STW) tornados.

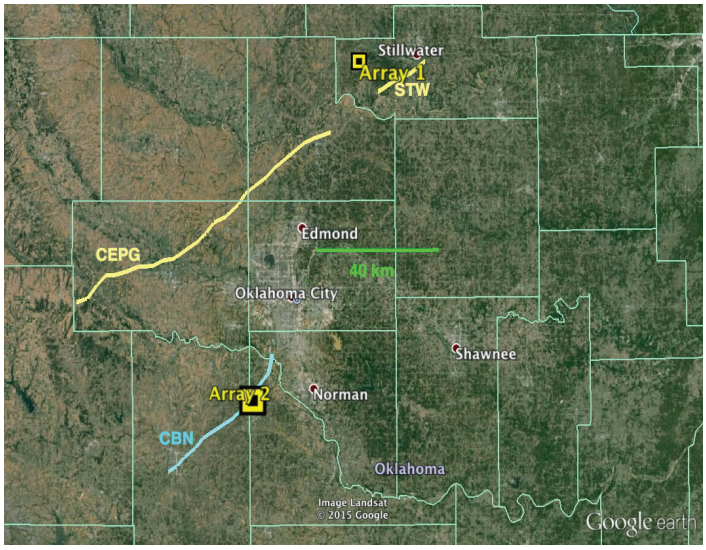

Figure 6. *Array locations and main storm tracks.*

Table 1: *Major tornados in Oklahoma during the May 24, 2011, outbreak; also included is the Stillwater tornado. Data are from the Norman OK National Weather Service Forecast Office.*

Name	Scale	Time [GMT]	Duration [minutes]	Length [miles]	Width [yards]
Canton Lake	EF-3	15:20-15:43	23	13	880
Calumet-El Reno-Piedmont-Guthrie (CEPG)	EF-5	20:50-22:35	105	63	1760
Chickasha-Blanchard-Newcastle (CBN)	EF-4	22:07-23:01	54	33	880
Lookeba	EF-3	20:31-20:46	15	9	880
Stillwater (STW)	EF-2	22:50-23:05	15	19	880
Washington-Goldsby	EF-4	22:27-23:05	38	23	880

A severe EF-5 tornado (denoted as CPEG in **Table 1**) touched down south of Hinton, OK, and remained on the ground for 63 miles, taking approximately 105 minutes to cover this distance. A speed of 151 mph, the highest wind gust ever registered on an Oklahoma Mesonet station[1], was generated by this tornado as it passed El Reno, OK. Approximately 15 minutes after the CPEG tornado lifted, a new EF-2 tornado (denoted STW) was spawned from a separate supercell and touched down south of Stillwater, OK, almost in line with the CPEG tornado. This tornado produced a 19-mile track and remained on the ground for 15 minutes.

[1] *The Oklahoma Mesonet is a network of 120 automated environmental monitoring stations developed by the University of Oklahoma and Oklahoma State University.*

Figure 7. *Array geometry for Array 1. The nominal location of this array was 36.10107°N, 97.26492°W, and is about 19 km west of Stillwater. The actual spacing between elements was closer to 500 m.*

Figure 8. *Array geometry for Array 2. The nominal location of this array was located at 35.19669°N, 97.65315°W in Blanchard, OK, and is about 35 km northwest of Chickasha, OK. As with Array 1, the actual spacing between elements was closer to 500 m.*

Through a combination of luck and good planning, Array 1 (shown in **Figure 7**) was optimally positioned to measure the infrasound from both tornados. As discussed below, the lifting of the CPEG tornado, followed after an interlude by a second less-intense tornado, provides clear evidence that infrasound and low-frequency sound detected during these tornado events are associated with the tornadic activity. The meteorology and infrasound/low-frequency propagation for Array 1 are discussed in Frazier et al. (2014) and they were very favorable for signal detection over the entire paths of the two tornados.

A third EF-4 tornado (denoted here as CBN) touched down just southwest of Chickasaw, OK, traveled a distance of 33 miles, and remained on the ground for 54 minutes. Array 2 was placed northeast of this tornado, and as shown in **Figure 8**, resulted in a near intercept of the tornado by the array with the closest point of approach of the core path ranging from 700 m to 1,200 m of the infrasound sensors. Unfortunately, the sensitivity of the sensors was too high for such a close-in approach, so a portion of the sensor recordings clipped when the tornado was near its point of closest approach.

Results from Array 1 for the CPEG and STW Tornados

The envelope of the pressure signal from element SN056 of Array 1 is shown in **Figure 9**. As illustrated, the level of sound increases as the CPEG tornado approaches, and there is a sudden drop in sound when the tornado lifts. After the new STW tornado spawns, sound levels again intensify until immediately after the dissipation of that tornado. Sound files from Array 1 for representative periods during this deployment are provided at http://acousticstoday.org/4162-2/.

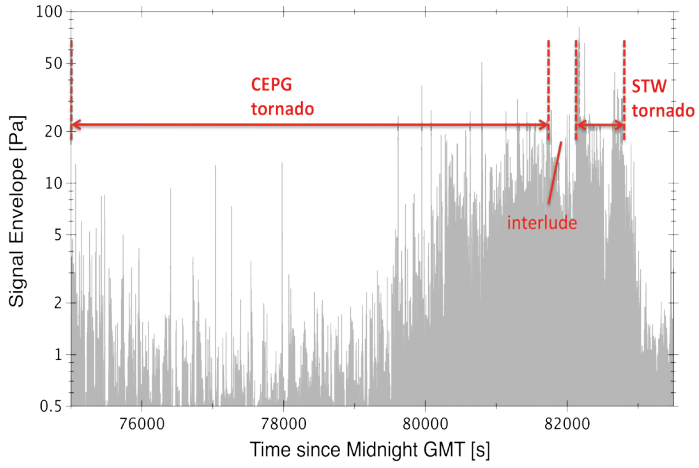

Figure 9. *Signal Envelope for SN056.*

Additional information can be gleaned by examining the waveform (**Figure 10**) over the period of the near approach by the CPEG tornado. What is observed, along with the expected strengthening of the signal, are intermittent noise bursts that are clearly coherent over the array. In addition, there are numerous smaller spikes during the period of closest approach. These are not coherent over the array, but a closer inspection of these spikes reveals a waveform resembling a damped sinusoidal oscillation with a period of about 200 to 300 Hz. Since this corresponds to the Helmholtz resonance of the sensor manifold, the likely explanation is that raindrops striking the top of the sensor caused it to ring at this characteristic frequency.

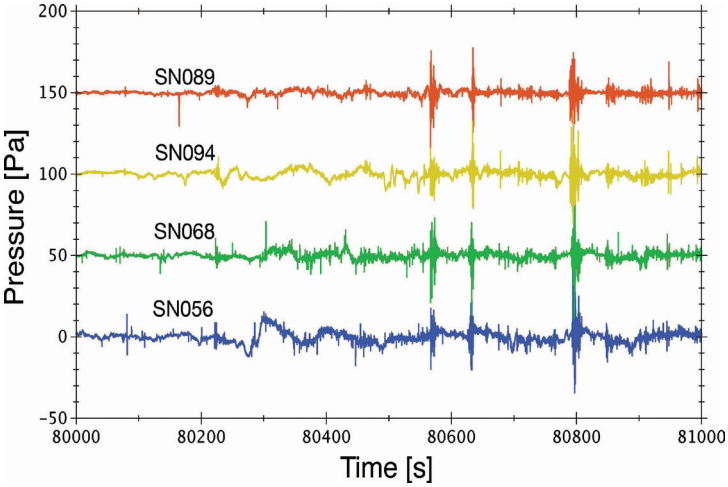

Figure 10. *Waterfall plot of signals from all elements of Array 1. The distance from the tornado increases upward.*

The most probable direction of arrival of the infrasound was estimated using a spatial filtering method called beam forming (e.g., Krim and Viberg, 1996). This processing was performed over the frequency region 0.5–3 Hz, and it relies on the infrasound remaining coherent over the infrasound array.

Coherent infrasound was not observed in the 0.5–2 Hz band reported by Bedard (2005). As pointed out previously, the array geometry was different for this array, which may account for he discrepancy between this and Bedard's previous work.

The beam-forming results for CPEG and STW are shown in **Figure 11**. We found the beam direction was within 10° of the direction of the estimated position of the tornado, which was consistent with our measurement uncertainty of the beam direction. Assuming the mechanism for producing the observed signal arrives from the tornado vortex, it is likely that more accurate tornado positions and beam directions would yield a net bias in the direction of propagation relative to the true direct of the tornado. This is because the circulation around the tornado will produce a bending of the propagation of the signal as it travels from the tornado vortex to the sensor. A similar effect has also been reported for large tropical cyclones (e.g., Blom, et al. 2014).

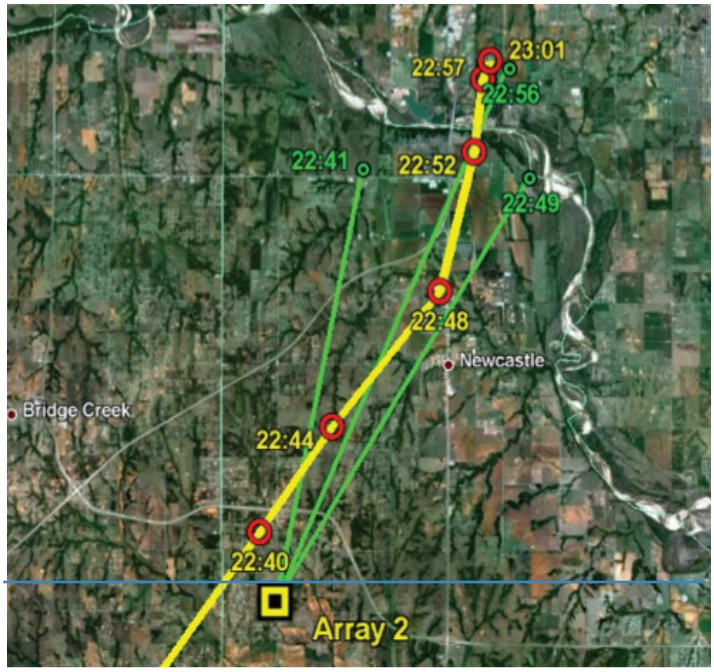

Figure 11. *Position of the CPEG and STW tornados at near approach as well as beam-forming rays (light blue). The time values by each beam-forming ray are the center times at which the beam direction was computed.*

Results from Array 2 for the CBN Tornado

As described previously, the CBN tornado path was very close to Array 2. As shown in Figure 16 of Frazier et al. (2014), the beam directions were in good agreement with the estimated tornado positions.

Spectral Analysis of the Infrasound Signals

The temporal patterns and array beam-forming results provide strong evidence that the origin of the infrasound and low frequency observed in the NCPA arrays were associated with the tornadic vortex. However, spectral analysis can yield insights into the mechanisms that generate this infrasound/low-frequency sound.

In **Figure 12,** we show the spectra as a function of time as the CPEG tornado approaches Array 1. The predominant feature observed is the rising high-frequency (80–100 Hz) shoulder as the tornado approaches. The lifting of the high-frequency tail above 150 Hz is probably associated with the onset of precipitation at the infrasound array. This feature

is seen across all results. For the STW and CBN tornados, the shoulder diminishes as the tornado moves away from the arrays. Furthermore, during the interlude between the CPEG and STW tornados, this high-frequency shoulder is conspicuously absent (the high-frequency tail thought to be associated with precipitation is still present however).

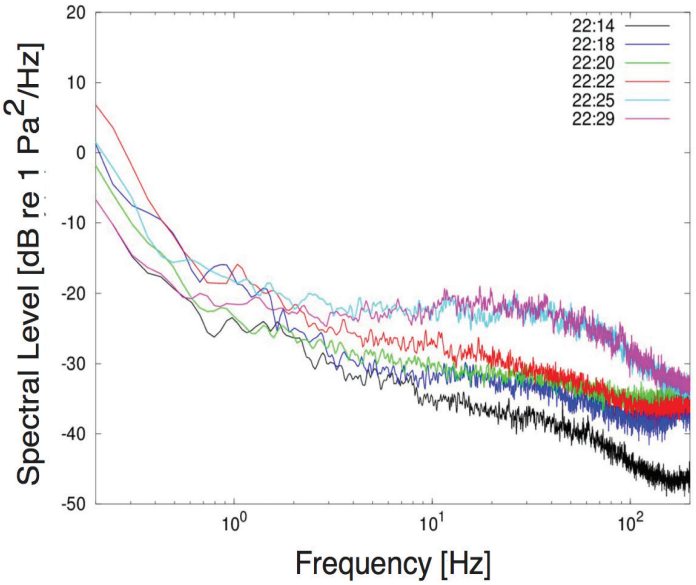

Figure 12. *Spectra as a function of time as the CPEG tornado approaches Array 1.*

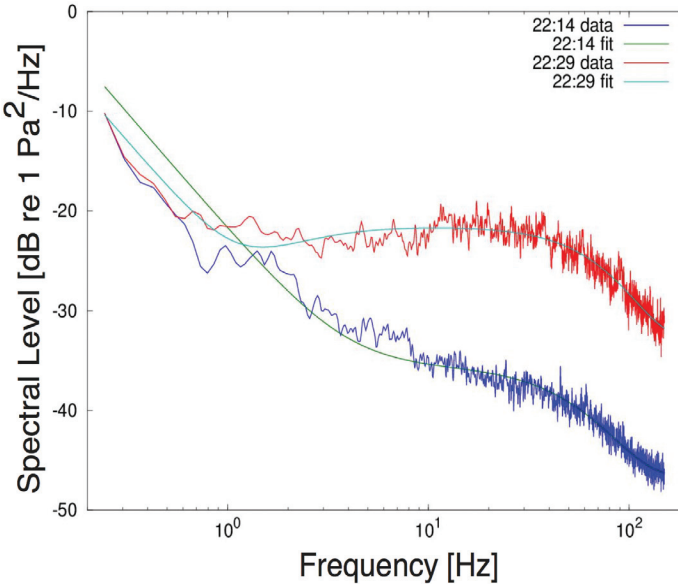

Figure 13. *Measured spectra and best fits using the model from Equation 1.*

This pattern of a larger high-frequency shoulder when the tornados are nearby is consistent with the mechanism of generation being associated with the tornadic vortex. As described in Frazier et al. (2014), a number of candidate mechanisms were considered. The only mechanism for this shoulder that we found to be consistent with the observations was sound generated by vortex emissions.

The model we used was based on a jet turbulence model by Powel (1959) with terms added to account for the bandwidth nature of the observed turbulence as well as losses associated with absorption and propagation of the sound

$$S(\omega,r) = A_f \omega^{-7/3} + \frac{A_s \omega_n^2 \omega^2}{\omega^4 + 4\zeta^2 \omega_n^2 \omega^2 + \omega_n^4} g_a(\omega,r) + A_n \quad (1)$$

In more detail, **Equation 1** models the power spectrum as the sum of a $\omega^{-7/3}$ power term associated with Kolmogorov inertial-subrange turbulence (e.g., Shields, 2005). The second term is the jet turbulence model, which has been modified to include a parameter ζ that controls the width of the peak and a g_a product that models the effects of attenuation and the propagation losses in the atmosphere (Bass et al. 1995). Example results of this fit are shown in **Figure 13**. As discussed further in Frazier et al. (2014), we were consistently able to accurately model all of the available spectra data using the model in **Equation 1**.

Summary

We have provided evidence that tornado vortices produce a characteristic spectral signature. Analogous to the "hook region" used by Doppler radar systems, it is possible that this characteristic spectral signature could be used in conjunction with permanent infrasound arrays to augment existing early warning systems. Clearly, more research would need to be done to establish the viability of such a system. Nonetheless, we believe these research results offer a promising new direction for further improvements in public safety.

Acknowledgments

We would like to acknowledge the employees at Hyperion Technology Group, LLC for their substantial contributions to this work. This work was funded by the National Oceanographic and Atmospheric Administration.

Biosketches

Carrick Talmadge was born in Richmond, IN. He received a BS in Physics from Saint Vincent College in 1981 and a PhD at Purdue University in 1987, focusing on experimental gravitational physics. His thesis advisor was Ephraim Fischbach. He remained on staff at Purdue before transferring to the University of Mississippi in 1998. He has worked on a variety of areas in science, including experimental gravity research, astrophysics, hearing science, low-frequency sound, infrasound, and metrological sciences (including calibration and sensor design).

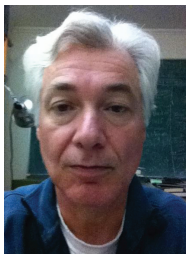

Roger Waxler was born and raised in New York City. He received a BA in Mathematics from the University of Chicago and a PhD in Physics from Columbia University, working on theoretical solid state physics with J. M. Luttinger. He began research on acoustics while visiting Penn State University and then accepted a position in the National Center for Physical Acoustics (NCPA) at the University of Mississippi. At the NCPA he has been specializing in acoustic phenomena and propagation in the atmosphere.

References

Abdullah, A. J., (1966). The 'musical' sound emitted by a tornado. *Monthly Weather Review* 94, 213–220.

Arnold, R. T., Bass, H. E., and Bolen, L. N. (1976). Acoustic spectral analysis of three tornadoes. *Journal of the Acoustical Society of America* 60, 584–593.

Bass, H. E., Sutherland, L. C., Zuckerwar, A. J., Blackstock, D. T., and Hester, D. M. (1995). Atmospheric absorption of sound: Further developments. *Journal of the Acoustical Society of America* 97, 680–683.

Bedard, Jr., A. J. (2005). Low-frequency atmospheric acoustic energy associated with vortices produced by thunderstorms. *Monthly Weather Review* 133, 241–263.

Bedard, Jr., A. J., and Georges, T. M. (2000). Atmospheric infrasound. *Physics Today* 53, 32–37.

Blom, P., Waxler, R., Frazier, W. G., and Talmadge C. (2014). Observations of the refraction of microbaroms generated by large maritime storms by the wind field of the generating storm. *Journal of Geophysical Research: Atmospheres* 119, 7179–7192.

Bluestein, H. (1999). *Tornado Alley: Monster Storms of the Great Plains*, Oxford University Press, New York.

Buhayar, N. (2011). *Joplin Tornado Leads Storms That May Cost Insurers $7 Billion in One Week.* Bloomberg, June, 2011. Available at http://www.bloomberg.com/news/articles/201106-06/joplin-tornado-leads-storms-that-may-cost-insurers-7-billion-in-one-week.

Fee, D., and Matoza, R. S. (2013). An overview of volcano infrasound: From Hawaiian to plinian, local to global. *Journal of Volcanology and Geothermal Research* 249, 123–139.

Frazier, W. G., Talmadge, C., Park, J., Waxler, R., and Assink, J. (2014). Acoustic detection, tracking, and characterization of three tornadoes. *Journal of the Acoustical Society of America* 135, 1742-1751.

Georges, T. M. (1973). Infrasound from convective storms: Examining the evidence. *Reviews of Geophysics* 11, 571–594.

Georges, T. M. (1976). *Infrasound from convective storms. Part II: A critique of source candidates.* NOAA Technical Report ERL 380-WPL 49, NOAA Environmental Research Laboratories, Boulder Colorado. Available at http://babel.hathitrust.org/cgi/imgsrv/download/pdf?id=psia.ark%3A%2F13960%2Ft6nz9gz8m;orient=0;size=100.

Kelly, D. L., Schaefer, J. T., McNulty, R. P., and Doswell III, C. A. (1978). An augmented tornado climatology. *Monthly Weather Review* 106, 1172–1183.

Krim, H., and Viberg, M. (1996). Two decades of array signal processing research: The parametric approach. *IEEE Signal Processing Magazine* 13, 67–94.

Mitchell, E. D. (1998). The National Severe Storms Laboratory tornado detection algorithm. *Weather and Forecasting* 13, 352–366.

Powell, A. (1959). Similarity and turbulent jet noise. *Journal of the Acoustical Society of America* 31, 812–813.

Raveloson, A., Kind, R., Yuan, X., and Ceranna, L. (2012). Locating the Tohoku-Oki 2011 tsunami source using acoustic-gravity waves. *Journal of Seismology* 16, 215–219.

Schecter, D. A. (2012). In search of discernible infrasound emitted by numerically simulated tornadoes. *Dynamics of Atmospheres and Oceans* 57, 27–44.

Shields, F. D. (2005). Low-frequency wind noise correlation in microphone arrays. *Journal of the Acoustical Society of America* 117, 3489–3496.

Stull, R. B. (1995). *Meteorology Today for Scientists and Engineers.* Brooks Cole, Belmont, CA.

Waxler, R., and Gilbert, K. (2006). The radiation of atmospheric microbaroms by ocean waves. *Journal of the Acoustical Society of America* 119, 2651–2664.